X-ray Crystal Structures Reveal Two Activated States for RhoC[†,‡]

Sandra M. G. Dias[§] and Richard A. Cerione*[,§,||]

Department of Molecular Medicine, College of Veterinary Medicine, and Department of Chemistry and Chemical Biology, Cornell University, Ithaca, New York 14853

Received January 8, 2007; Revised Manuscript Received March 29, 2007

ABSTRACT: RhoC is a member of the Rho family of Ras-related (small) GTPases and shares significant sequence similarity with the founding member of the family, RhoA. However, despite their similarity, RhoA and RhoC exhibit different binding preferences for effector proteins and give rise to distinct cellular outcomes, with RhoC being directly implicated in the invasiveness of cancer cells and the development of metastasis. While the structural analyses of the signaling-active and -inactive states of RhoA have been performed, thus far, the work on RhoC has been limited to an X-ray structure for its complex with the effector protein, mDia1 (for mammalian Diaphanous 1). Therefore, in order to gain insights into the molecular basis for RhoC activation, as well as clues regarding how it mediates distinct cellular responses relative to those induced by RhoA, we have undertaken a structural comparison of RhoC in its GDP-bound (signaling-inactive) state versus its GTP-bound (signaling-active) state as induced by the nonhydrolyzable GTP analogues, guanosine 5′-(β,γ-iminotriphosphate) (GppNHp) and guanosine 5′-(3-*O*-thiotriphosphate) (GTPγS). Interestingly, we find that GppNHp-bound RhoC only shows differences in its switch II domain, relative to GDP-bound RhoC, whereas GTPγS-bound RhoC exhibits differences in both its switch I and switch II domains. Given that each of the nonhydrolyzable GTP analogues is able to promote the binding of RhoC to effector proteins, these results suggest that RhoC can undergo at least two conformational transitions during its conversion from a signaling-inactive to a signaling-active state, similar to what has recently been proposed for the H-Ras and M-Ras proteins. In contrast, the available X-ray structures for RhoA suggest that it undergoes only a single conformational transition to a signaling-active state. These and other differences regarding the changes in the switch domains accompanying the activation of RhoA and RhoC provide plausible explanations for the functional specificity exhibited by the two GTPases.

Members of the Rho family of the Ras superfamily of GTPases[1] act as molecular switches that cycle between GDP-bound ("off") and GTP-bound ("on") states to regulate cell shape, polarity, cytokinesis, and locomotion (*1*). The three best studied members of the Rho family, RhoA, Rac1, and Cdc42, have taken center stage primarily because they were the first to be described as playing important roles in rearrangements of the actin cytoskeleton and in the morphological responses of cells to extracellular stimuli. RhoA, which represents the founding member of the Rho family, shares high sequence homology (∼85%) with RhoB and RhoC. However, thus far, distinct cellular functions have not been assigned to these different isoforms (*2*). Perhaps the clearest indication that differences exist in the cellular activities mediated by the individual Rho proteins comes from studies of human cancer. The Rho proteins play important roles in many aspects of malignant transformation, and each member of the Rho family may be involved to varying degrees at different stages of tumor progression (*3*). RhoA and RhoB have been shown to promote the transformation of cultured mouse fibroblasts, and these transformed cells were tumorigenic when injected into mice (*4*−*6*), whereas RhoC was identified as a key regulator of migration and metastasis in human melanoma and breast cancer cell lines (*3*, *7*, *8*). The serine/threonine kinase ROCK was initially identified as a target for RhoA (*9*); however, RhoC may be the better activator (*10*), perhaps accounting for its potential involvement in metastatic cancers, especially given that the activation or inhibition of ROCK, respectively, promotes or inhibits tumor cell motility (*10*, *11*). Protein interaction studies suggest that both ROCK and another Rho-family effector, Citron, have a higher affinity for RhoC compared to RhoA and RhoB (*2*). Other Rho-family effectors like Rhophilin and PKC-ϵ also display differential affinity for RhoA and RhoC as indicated in pull-down assays and yeast two hybrid experiments (*2*).

Most of the differences between the amino acid sequences of RhoA, RhoB, and RhoC occur within their C-terminal ends. Each of the Rho proteins are posttranslationally modified by the prenylation of a conserved C-terminal cysteine residue followed by methylation and proteolytic removal of the last three amino acids. These modifications are important for anchoring the Rho proteins to membranes, as well as for their stability (*12*, *13*). The N-terminal halves

[†] This work was supported by NIH Grants EY06429 and GM47458.

[‡] Atomic coordinates and diffraction data are available in the Protein Data Bank at www.rcsb.org (PDB codes 2GCN, 2GCO, and 2GCP).

* To whom correspondence should be addressed. E-mail: rac1@cornell.edu. Tel: (607) 253-3888. Fax: (607) 253-3659.

[§] Department of Molecular Medicine.

[||] Department of Chemistry and Chemical Biology.

[1] Abbreviations: GTPase, guanosine triphosphatase; PEG 3350/8000, polyethylene glycol 3500/8000; GAP, GTPase-activating protein; PKN, protein kinase N; ROCK, Rho kinase; GTPγS, guanosine 5′-(3-*O*-thiotriphosphate); mDia1, mammalian Diaphanous 1; GppNHp, guanosine 5′-(β,γ-iminotriphosphate); GppCH$_2$p, guanosine 5′-(β,γ-methylenetriphosphate); rmsd, root-mean-square deviation.

10.1021/bi700035p CCC: $37.00
Published on Web 05/12/2007

of the Rho proteins contain the majority of the residues necessary for GTP-binding and hydrolytic activities, together with the switch I and II regions that change conformation between the GTP-bound and GDP-bound states. Amino acids essential for these catalytic functions are conserved in all three Rho isoforms. Some sequence divergence between RhoA, RhoB, and RhoC is found in the insert loop, a helical region comprised of 15 amino acids (residues 123−137) that is present in most Rho-family members but not in other Ras-superfamily GTPases (*2*). Effector proteins that uniquely interact with the insert loop of RhoA, RhoB, or RhoC have not been identified, although deletion of this region from RhoA causes a decrease in protein stability and a reduction in its transforming potential (*14*) by compromising its ability to activate Rho kinase (*15*). The differences that exist in the insert regions of the different Rho proteins might help to account for their differential abilities to interact with specific regulators or targets.

Several high-resolution X-ray crystallographic structures have been determined for RhoA bound to GDP and GTP analogues, as well as to different regulatory and effector proteins. However, thus far, the only X-ray crystal structure available for RhoC is of its complex with the regulatory N-terminal portion of mDia1 containing the GBD/FH3 region, an all-helical structure with armadillo repeats (*16*). No comparative structural information has yet been available in order to verify conformational differences between the signaling-inactive, GDP-bound form of RhoC and its signaling-active, GTP-bound state. Perhaps more importantly, a question remains as to whether there is any structural distinction between RhoA and RhoC that could account for the differences in their abilities to bind effectors. Here we show for the first time a structural comparison of the signaling-inactive and signaling-active states of RhoC. We use these findings to gain insights into the nature of the conformational changes that are necessary for RhoC to assume a signaling-active state. We also compare the RhoC structures that we have determined with those reported for RhoA, as well as the RhoC−mDia1 complex, in order to better understand the functional differences exhibited by the RhoA and RhoC proteins.

EXPERIMENTAL PROCEDURES

Protein Expression and Purification of RhoC. Similar to the structural studies of other small GTPases, we constructed a truncated form of the human RhoC protein (residues 1−181) in which 12 C-terminal residues were deleted. This construct (referred to hereafter as RhoC) was cloned into pET28a(+) (Novagen) and used to transform *Escherichia coli* BL21(DE3) (Stratagene) cells. The cells were lysed, and the clarified soluble fraction was incubated with either 250 μM GDP or GppNHp (Sigma Aldrich) per liter of culture. A two-step purification was performed, starting with IMAC using the Co^{2+}-charged TALON resin (BD Biosciences), equilibrated with 20 mM Hepes-Na, pH 8.0, 500 mM NaCl, 5 mM imidazole, 0.3 mM TCEP [tris(2-carboxyethyl)-phosphine hydrochloride], and a cocktail of protease inhibitors. The protein was eluted with 300 mM imidazole. A Hiload Superdex 200 16/60 gel filtration column (GE Healthcare), equilibrated in 20 mM Hepes-Na, pH 8.0, 5 mM $MgCl_2$, and 5 mM DTT, was used for the final step of the purification procedure. The eluted protein was concentrated and either frozen with liquid nitrogen (after the addition of 20% glycerol) and stored at −80 °C or immediately used for crystallization screens. To obtain crystals for the RhoC−GppNHp and RhoC−GTPγS complexes, a 20-fold molar excess of each nucleotide was added to the final protein solution. Protein concentrations were determined by the Bradford method (Bio-Rad kit) using BSA as a standard.

Crystallization and Data Collection/Processing. Crystals for the RhoC complexes were obtained by using the conventional hanging-drop vapor diffusion technique. The initial conditions were screened at 18 °C, using the Crystal Screen, Crystal Screen 2, and Index kits from Hampton Research. Collected crystals were obtained at the optimized conditions of 100 mM BisTris, pH 6.0, and 20% PEG 3350 (RhoC−GDP); 100 mM sodium cacodylate, pH 6.4, 200 mM sodium acetate, and 30% PEG 8000 (RhoC−GppNHp); and 100 mM sodium acetate, pH 4.8, and 3 M NaCl (RhoC−GTPγS). Drops were prepared by mixing equal parts of protein and the well solution, with the initial protein concentration being 10−20 mg/mL. Crystals could be observed in about 24 h. Before data collection at cryogenic temperature (100 K), crystals were soaked in cryoprotectant solution containing the mother solution prepared with 10%, 15%, or 20% ethylene glycol for RhoC−GDP, RhoC−GppNHp, and RhoC−GTPγS, respectively. The X-ray diffraction data sets for RhoC−GDP and RhoC−GTPγS were obtained using a Rigaku RTP 300 RC copper rotating anode X-ray generator operating at 50 kV and 100 mA, equipped with a Rigaku RAXIS IV++ image plate detector. The Cornell High-Energy Synchrotron Source (CHESS) station F2 was used to collect the RhoC−GppNHp data set, using a Quantum 210 X-ray detector (Area Detector Systems Corp.). Data were processed using MOSFLM (*17*) and scaled with SCALA (*18*).

Phasing and Refinement. The first set of phases was obtained by the molecular replacement technique implemented in the program Molrep (*19*), searching for one (RhoC−GDP and RhoC−GTPγS data sets) or two (RhoC−GppNHp) protein molecules in the asymmetric unit, as predicted by the Matthews coefficient (*20*). A monomer of the human RhoC structure was used as the search model [Protein Data Bank, PDB ID 1Z2C (*16*)]. Rigid-body refinement followed by subsequent cycles of positional and *B*-factor refinements was carried out with Refmac (*21*). Real space refinement, through inspection of the Fourier electron density maps, was performed with Coot (*22*). Cycles of TLS were applied as the final steps of the refinement using Refmac (*21*). Solvent water molecules, treated as oxygen atoms, were added using the Coot routine. During model refinement, the analysis of Fourier difference maps indicated the presence of very strong electron densities (over 3σ in height), both inside the canonical nucleotide-binding site and the Mg^{2+} sites, for each monomer in the asymmetric unit. The overall stereochemical quality of the final model and the agreements between model and experimental data were assessed by both the program PROCHECK (*23*) and proper Coot tools.

RESULTS

Overall Structural Features. The X-ray crystal structures for the human RhoC protein bound to GDP, GppNHp, and

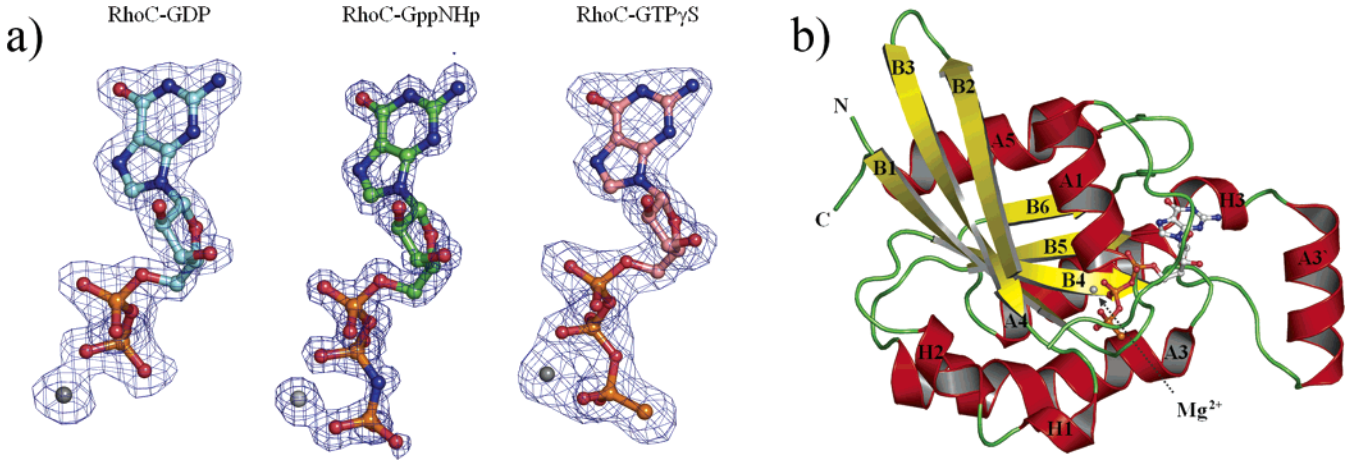

FIGURE 1: Structure of RhoC bound to different guanine nucleotides. (a) Omit electron density maps $F_o - F_c$ (in blue) for the nucleotides and Mg^{2+} ions, contoured at sigma level 3 are, from left to right, GDP (cyan), GppNHp (green), and GTPγS (salmon). (b) Ribbon diagram for RhoC complexed with GTPγS. The β-strands are in yellow, helices are in red, and loops are in green. The bound nucleotide is shown as a ball and stick model and the Mg^{2+} ion as a gray sphere.

Table 1: Parameters and Statistics of Diffraction Data and Refinement[a]

parameters	GDP	GppNHp	GTPγS
data collection			
space group	$P2_12_12_1$	$P2_12_12$	$P4_32_12$
unit cell *a*, *b*, *c* (Å)	44.2, 56.6, 81.8	64.1, 75.6, 82.9	59.4, 59.4, 138.1
asymmetric unit	1 molecule	2 molecules	1 molecule
resolution range (Å)	26.5−1.85 (1.95−1.85)	30.32−1.4 (1.48−1.4)	54.55−2.15 (2.2−2.15)
no. of unique reflections	17803 (2369)	75377 (11027)	14205 (2019)
average multiplicity	3.4 (2.4)	5.0 (4.8)	11.8 (11.9)
completeness (%)	98.3 (91.2)	95.0 (96.2)	100 (100)
R_{sym} (%)	5 (14.8)	8.5 (50.8)	12.2 (58.3)
$\langle(I)/\sigma(I)\rangle$	20.6 (6.0)	13.1 (3.0)	19.1 (3.8)
refinement			
resolution range	26.5−1.85	8.00−1.4	54.55−2.15
total no. of reflections used	16860	71246	13442
no. of reflections for R_{free} calcd	905	3768	710
R_f (%)	17.6	19.7	15.9
R_{free} (%)	22.5	22.0	22.6
rmsd from ideal bond length (Å)	0.014	0.009	0.016
rmsd from ideal angle (deg)	1.604	1.352	1.733
Ramachandran plot			
most favored regions (%)	92.3	93.1	93.6
permitted regions (%)	7.7	6.9	6.4

[a] Numbers in parentheses refer to the highest resolution shell.

GTPγS were determined at 1.85, 1.4, and 2.15 Å resolution, respectively. The space groups together with the summary of the structure refinements and the final model statistics for the different complexes are presented in Table 1. In each of the three RhoC complexes, the electron density map unambiguously shows the presence of the specific guanine nucleotide and a Mg^{2+} ion. Figure 1a shows representative σ-weighted $F_o - F_c$ composite omit maps for each of the different RhoC structures, calculated at the final stage of refinement. In the case of the RhoC−GTPγS complex, the $2F_o - F_c$ electron density map for the γ-phosphate coordination showed that one of the atoms had a bulkier electron density compared to the other two atoms. A sulfur atom could be placed there with an occupancy equal to 1 and a final *B*-factor value of 11.84, in good agreement with the overall *B*-factor for the ligand (i.e., an average value of 11.64).

The three RhoC complexes have very similar structures. The superposition of Cα atoms (i.e., the alignment between Ala3 and Leu179) for the RhoC−GDP complex onto the RhoC−GppNHp (chain A) and RhoC−GTPγS complexes, as performed by LsqKab (*24*), yielded rms deviations of 0.91 Å (with a maximum value of 6.4 Å) and 1.55 Å (with a maximum value of 6.68 Å), respectively, while the superposition of the RhoC−GppNHp complex onto the RhoC−GTPγS complex gave a rmsd value of 1.37 Å (maximum value of 6.88 Å). The main features of the fold for each of the RhoC complexes, consisting of a six-stranded β-sheet surrounded by five α-helices, are basically the same as those found in other related small GTPases (*25*), as shown by the ribbon diagram for the RhoC−GTPγS complex in Figure 1b. The bound guanine nucleotides undergo extensive hydrophobic and hydrophilic interactions with the surrounding residues, and the Mg^{2+} ion is coordinated by six oxygens in an octahedral geometry, again similar to what has been observed for other small GTPases in their complexes with GTP, GTP analogues, or GDP (*25*, *26*). No significant differences were observed between the GDP-, GppNHp-, and GTPγS-bound forms of RhoC; Figures 2a and 2b compare the nucleotide-binding interactions for the RhoC−GppNHp- and RhoC−GTPγS-bound complexes. As will be described

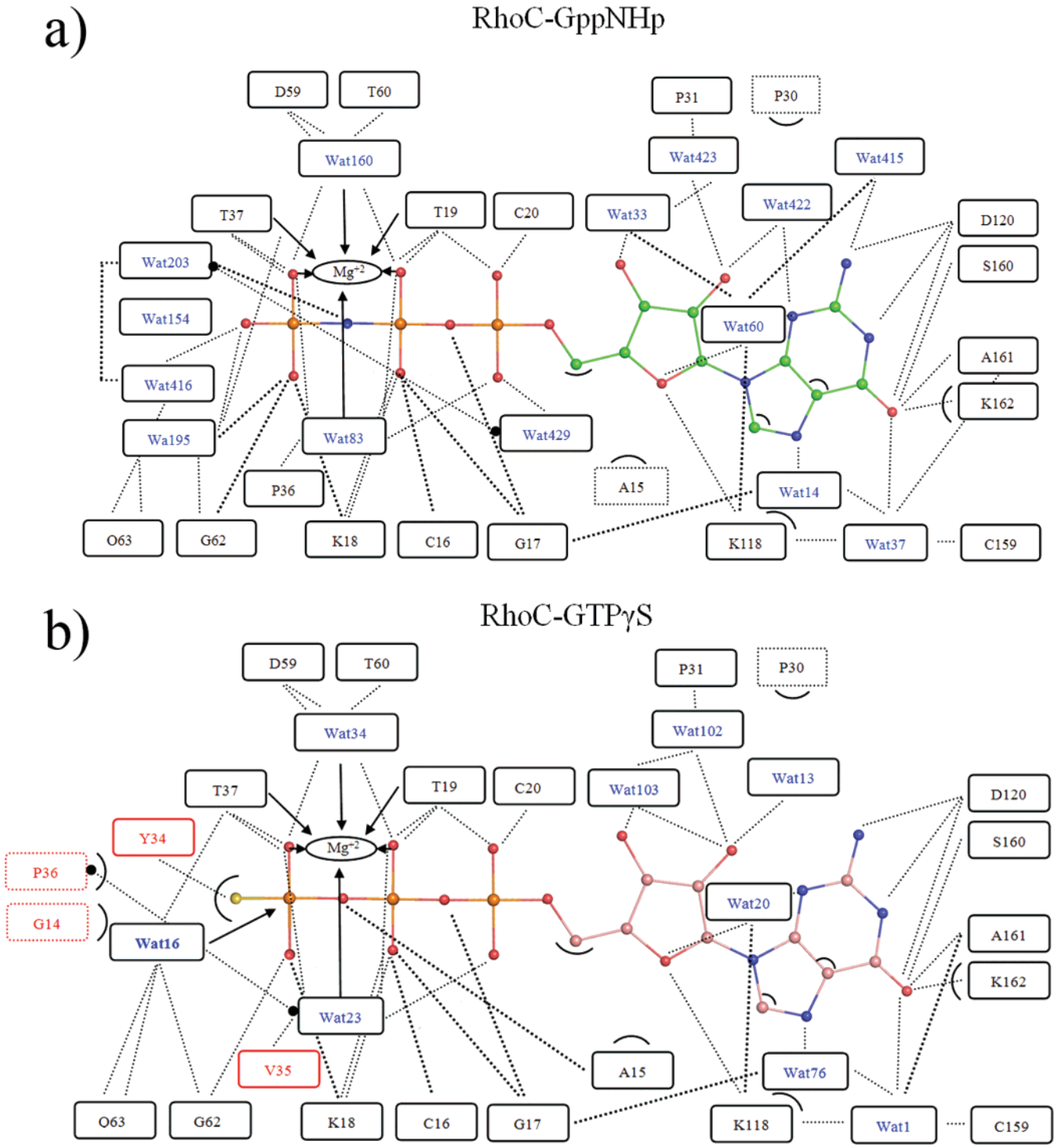

FIGURE 2: Interactions of GppNHp and GTPγS with RhoC. Polar and apolar interactions of GppNHp (a) and GTPγS (b) with RhoC, Mg^{2+}, and water molecules were defined by PyMOL (*52*). All dashed lines correspond to hydrogen-bonding interactions (distance less than 3.5 Å), the arrows represent Mg^{2+}−residue/water contacts, and the half-circles represent hydrophobic interactions (distance less than 3.9 Å). Residues and water molecules are represented by rectangles (written in blue for the water molecules), Mg^{2+} by an ellipsoid, and ligands as ball and stick models (blue for nitrogen, red for oxygen, green or salmon for carbon, yellow for sulfur, and orange for phosphorus). Residues involved in interactions with the nitrogen base and pentose sugar are the same between the GppNHp− and GTPγS−RhoC complexes. The same protein−phosphate interactions are also present in both the RhoC−GppNHp and −GTPγS structures (Cys16, Gly17, Lys18, Thr19, Cys20, Thr37, Gly62, Gln63), although the RhoC−GTPγS complex has more interacting residues (Gly14, Tyr34, Val35, Pro36, boxes in red) and less interacting water molecules.

further below, the main differences between the RhoC complexes were evident in the switch I and II regions.

Differences in the Interactions between Guanine Nucleotides and the Switch Domains for the GDP-, GppNHp-, and GTPγS-Bound RhoC Complexes. Some differences begin to emerge when examining the interactions between the guanine nucleotides and the switch domains for the different RhoC complexes. While the interactions between the switch I domain (Lys27−Tyr42) and the bound guanine nucleotide are basically the same for the RhoC−GDP and RhoC−GppNHp complexes, some prominent differences are observed between RhoC−GppNHp and RhoC−GTPγS. For

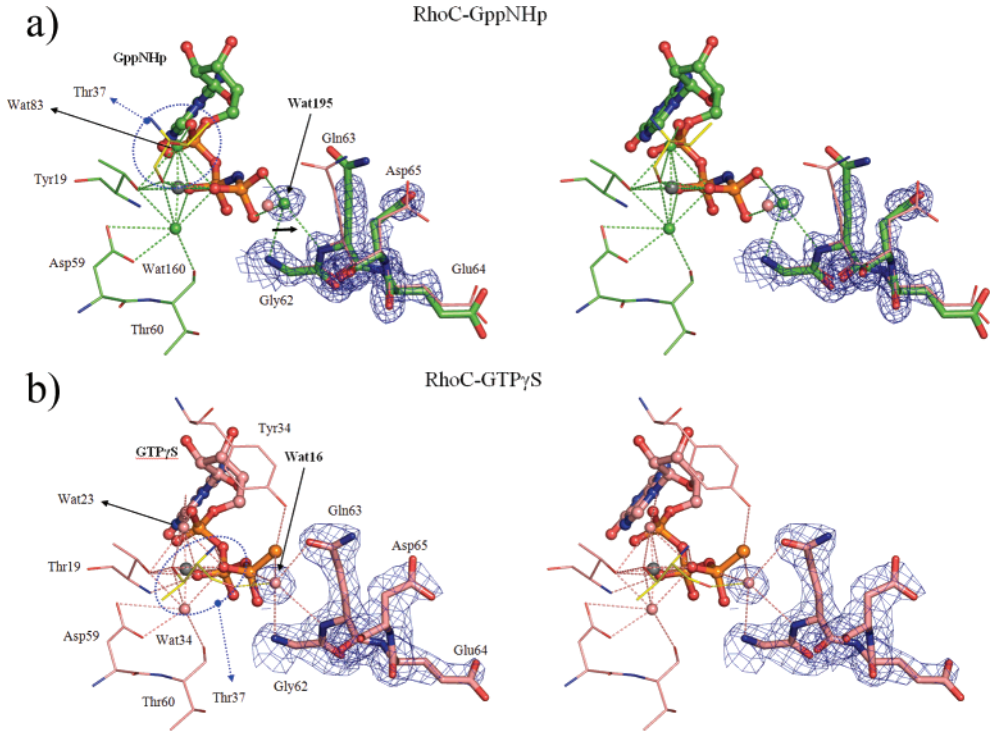

FIGURE 3: RhoC residues involved in binding the γ-phosphate of GTP analogues. Ball and stick representation of GppNHp (a) and GTPγS (b) and their interactions with Mg^{2+} (gray sphere), as well as with water molecules from the Mg^{2+} octahedral coordination (salmon or green spheres), the proposed catalytic water [Wat16 in (b)], and residues (Thr19, Thr37, Asp59, and Thr60) (drawn as lines) involved in the coordination of Mg^{2+}. Other indicated residues are Tyr34, which contacts the sulfur atom [(b), orange ball at the extremity], and Gln63, Glu64, and Asp65 (represented by sticks) along with their $2F_o - F_c$ density map. The $2F_o - F_c$ density map is also shown for Wat16 and Wat195. Hydrogen bonds are represented by dotted lines, and Thr37 is colored yellow and circled by a blue dotted line to emphasize the displacement of this residue, when comparing both structures. The hydrogen bond to the potential catalytic water [represented by a yellow dotted line in (b)] is lost in the RhoC−GppNHp structure. In (a) Wat16, Gln63, Glu64, and Asp65 (all in salmon, residues represented by lines) from RhoC−GTPγS are superposed to the RhoC−GppNHp structure (in green, stick representation for the same residues). The small thick arrow indicates the dislocation of the proposed catalytic water by 1.05 Å to its position (Wat195) within the RhoC−GppNHp complex.

example, Tyr34 of RhoC makes a hydrogen bond with the sulfur atom of GTPγS, whereas this same tyrosine is positioned away from the nucleotide and has a poorly defined electron density in the RhoC−GppNHp structure. The main-chain carboxylic oxygen of Pro36 makes a hydrogen bond with a water molecule that contacts the Mg^{2+} ion within both RhoC complexes; however, its side-chain ring only makes hydrophobic contact with the nucleotide sulfur atom in the RhoC−GTPγS complex (Figure 2). Despite the fact that Thr37 occupies distinct positions in the X-ray structures for the RhoC complexes with the two GTP analogues, it participates through its side-chain carboxyl in Mg^{2+} coordination within the GTPγS-bound complex and via its main-chain carboxyl within the GppNHp-bound complex (Figure 3). However, the displacement of Thr37 in the RhoC−GppNHp-bound complex, compared to its position in the GTPγS-bound complex, prevents the formation of a potentially important hydrogen bond to the catalytic water for the GTP hydrolytic reaction.

Within the switch II region of the RhoC−GTPγS and RhoC−GppNHp structures (Asp59−Asp78), Asp59 and Thr60 are hydrogen-bonded to water (i.e., Wat34 and Wat160, respectively), with both water molecules being involved in coordinating the Mg^{2+} ion. The main-chain amide of Gly62 makes polar contacts with one of the γ-phosphate oxygens in both complexes, while Gln63 contacts the proposed catalytic water (Wat16) within the RhoC−GTPγS complex. This Gln residue indirectly contacts the γ-phosphate of GppNHp through a uniquely positioned water molecule (Wat195) that does not appear to be in the appropriate position to participate in the catalytic mechanism for GTP hydrolysis (Figure 2). GDP-bound RhoC shows the same Mg^{2+}-mediated contacts between Asp59, Thr60, and the nucleotide, as seen in the RhoC−GTPγS and RhoC−GppNHp complexes, although it lacks the Gly62 and Gln63 interactions as they are established through the γ-phosphate (data not shown). Indeed, these residues, along with a portion of switch II (Gly62−Ser73), exhibit higher *B*-factors, such that their average value is 5.5 Å^2 greater than the average *B*-factor for the GDP-bound RhoC structure (18.09 Å).

Differences in the Conformational Changes Accompanying Nucleotide Exchange between the Different RhoC Complexes and the Corresponding RhoA Complexes. Given the differences in the switch domain interactions with guanine nucleotides for the different forms of RhoC, we wanted to take a closer look at the conformational changes accompanying the conversion of RhoC from the GDP-bound state to the GTP-bound state. The RhoC−GDP complex exhibited a well-defined electron density map for switch I but a poorly defined map for some of the switch II residues, which likely reflects conformational disorder and/or the presence of internal thermal motions. Switch I is pulled away from the nucleotide in the RhoC−GDP complex and is stabilized by an intramolecular contact between Ile23 and Phe39 (Figure 4a). This switch conformation is identical to that observed for the RhoA−GDP complex and similar to the GDP-bound forms of Rac1 (*27*), Cdc42 (*28*), and H-Ras (*29*) (data not shown). Each of these complexes shows that Tyr34 (for

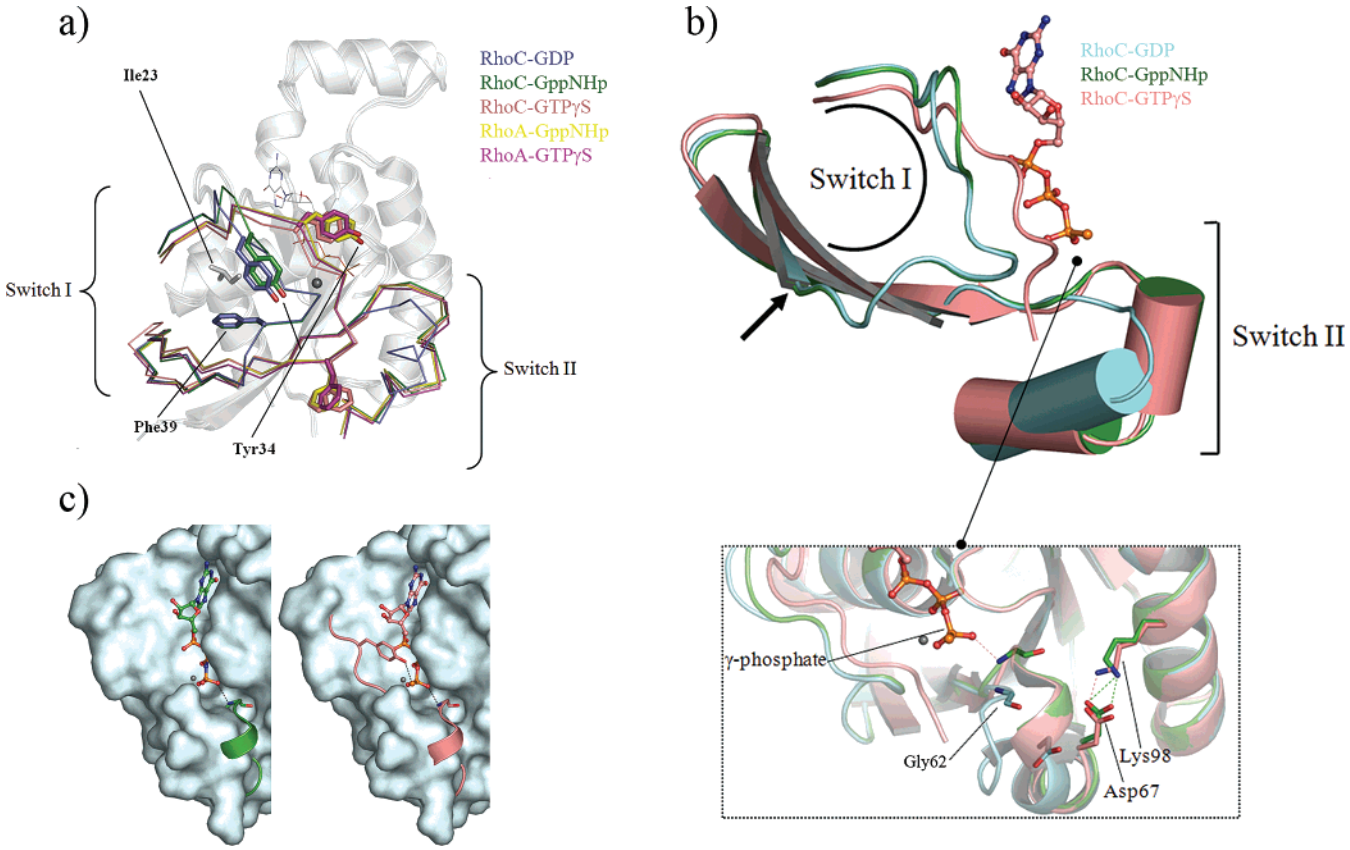

FIGURE 4: Comparisons between the GDP- and GTP-bound forms of RhoA and RhoC. (a) Superposition of the structures for GDP-, GTPγS-, and GppNHp-bound RhoC with RhoA−GppNHp (PDB ID 1KMQ) and RhoA−GTPγS (PDB ID 1A2B). The segment containing Asp28−Pro75 (switch I and switch II) is represented as a ribbon, with RhoC−GDP, RhoC−GppNHp, RhoC−GTPγS, RhoA−GppNHp, and RhoA−GTPγS shown in slate, green, salmon, yellow, and magenta, respectively. Ile23, Tyr34, and Phe39 are represented by sticks. The Mg^{2+} appears as a gray sphere. The switch I disposition of RhoC−GppNHp shows differences relative to the other three nucleotide-activated structures as it was unchanged from switch I in the GDP-bound state of RhoC. (b) Comparison of the segment containing Asp28−Pro75 (switch I and switch II) of RhoC complexed with GDP (cyan), GppNHp (green), and GTPγS (salmon). The Mg^{2+} is represented by a gray sphere. The inset shows a more detailed view of switch II and the hydrogen bond between the γ-phosphate of the GTP analogues and Gly62 (main chain) (dashed line). This interaction may be further stabilized by an intramolecular salt bridge between Asp67 and Lys98 (dashed lines). The arrow shows the position of Ile43, which may help to stabilize the partially activated state. (c) Superposition of the structure for the RhoC−GDP complex (shown in cyan as a van der Waals surface) with RhoC−GppNHp (left panel, green) and RhoC−GTPγS (right panel, salmon). The superposition shows the switch II movements due to the binding of the GTP analogues.

RhoC and RhoA; Tyr32 for Rac1, Cdc42, and H-Ras) is pulled away from the nucleotide. Interestingly, the RhoC−GDP and RhoC−GppNHp complexes exactly overlap within their switch I segments, while the RhoC−GTPγS complex shows a flipped-down conformation for switch I (Figure 4). In fact, the entire switch I region (Asp28−Val38) is positioned differently for the GTPγS-bound RhoC complex, compared to either the GDP- or GppNHp-bound forms of RhoC. In the RhoC−GTPγS complex, this region moves toward the GTP analogue and assumes a position that is stabilized by hydrophobic and hydrophilic interactions, including a hydrogen bond between Tyr34 and the γ-phosphate sulfur (also see Figure 2b). Therefore, as the switch I region is brought down in the RhoC−GTPγS complex, the side chain of Phe39 becomes exposed to the protein surface and is stabilized by a contact to another symmetry-related Phe39. The differences within the switch I regions result in the shortening of the β2-strand for the GDP- and GppNHp-bound states of RhoC (indicated by the arrow in Figure 4b), compared to the GTPγS-bound state. They also account for the fact that there are significantly fewer water molecules interacting with the γ-phosphate in the RhoC−GTPγS complex compared to the RhoC−GppNHp complex (Figure 2).

While switch II is relatively poorly defined in the GDP-bound state of RhoC, it exhibits a more stabilized structure in the GppNHp- and GTPγS-bound states. This change in switch II appears to be driven by the γ-phosphate, which, among other interactions, contacts the main-chain amide of Gly62 and may be stabilized by the salt bridge between Asp67 and Lys98 (Figure 4b). The new switch II conformation that accompanies the binding of the GTP analogues is also responsible for a topological difference between the GDP- and the GTP-bound states; namely, within the GDP-bound complex, the H1 and H2 3_{10}-helices come together to form one longer α-helix (Figure 4b).

The rmsd value obtained when superposing the Cα atoms (Ala3−Leu179) of GDP-bound RhoA (*30*) onto GDP-bound RhoC was 0.5 Å (maximum value of 2.56 Å), while the rmsd values for superposing GppNHp-bound RhoC and GTPγS-bound RhoC onto the corresponding complexes for RhoA (*25*, *31*) were 1.21 Å (6.62 Å maximum distance) and 0.55 Å (1.57 Å maximum distance), respectively. These values show that the structures for the switch regions of the GDP- and GTPγS-bound forms of RhoA are essentially identical to the corresponding structures for RhoC, whereas the switch I region for the GppNHp-bound form of RhoA differs from

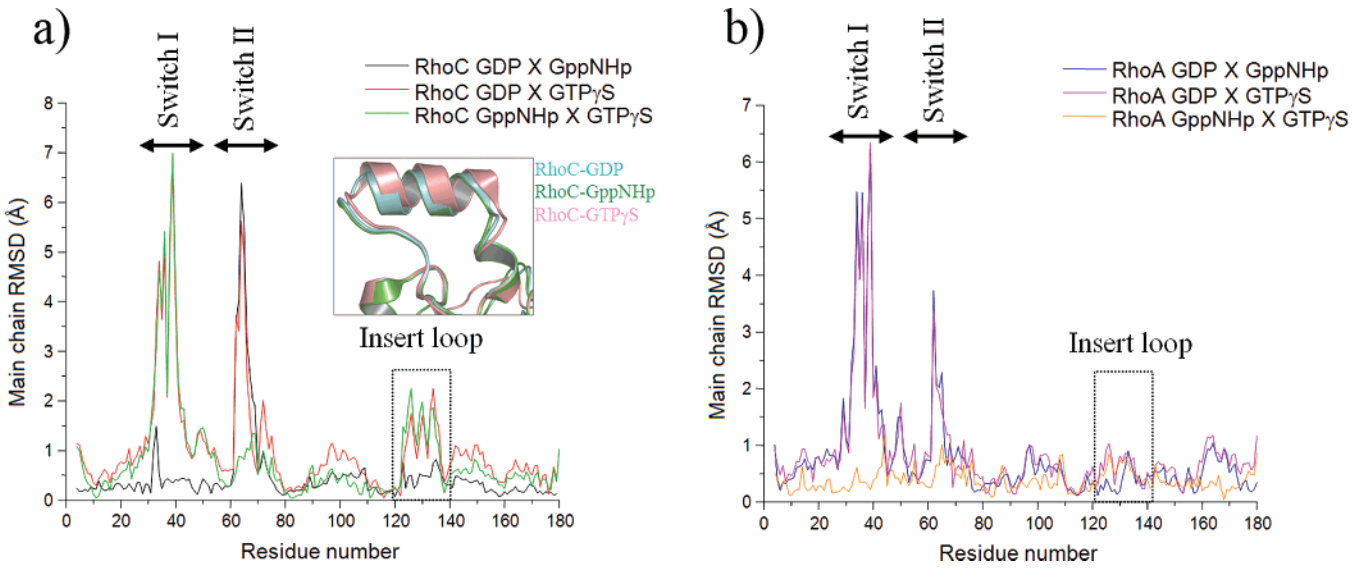

FIGURE 5: The X-ray crystal structure for RhoC−GTPγS shows considerable movement within the Rho-insert loop. The Cα rmsd for residues 4−180 of RhoC (a) and RhoA (b) crystallized with different guanine nucleotide analogues; the inset shows the deviation in the Rho-insert region RhoC−GTPγS (salmon) relative to the RhoC−GDP and RhoC−GppNHp complexes (cyan and green, respectively).

that for GppNHp-bound RhoC. In particular, in the RhoA−GppNHp complex, the switch I region has moved closer toward the GTP analogue, similar to what we see for the RhoC−GTPγS complex (Figure 4a).

Another intriguing difference between the RhoA and RhoC structures is an ~2 Å deviation between the Cα atoms of the insert loop (namely, residues Gln123−Glu137) when comparing the structures for the GDP- and GTPγS-bound forms of RhoC (Figure 5a). No difference for the insert region is evident when comparing the structures for RhoC−GDP and RhoC−GppNHp (Figure 5a) nor when comparing the complexes for RhoA bound to GDP versus GTP analogues (Figure 5b).

Implications for RhoC-Dependent Signaling. The structure for RhoC−GppNHp bound to mDia1 [PDB ID 1Z2C (*16*)] highlights the main elements responsible for this GTPase−effector interaction. The calculated solvent-accessible area buried per molecule is 1204.6 Å^2 for RhoC and 1271.2 Å^2 for mDia1, with only ~10% of the binding interface being contributed by switch I residues Val38, Phe39, and Glu40. Most of the remaining area is contributed by several switch II residues, with the majority of these residues being brought into the proper position for binding to the effector following the exchange of GDP for GppNHp. The interaction surface for mDia1 involves hydrophilic contacts with the RhoC switch II residues Gln63, Tyr66, Asp67, and Arg68, as well as with residues Glu102, His105, and Phe106. There also is a hydrophobic core from mDia1 that interacts with switch I residues Val38 and Phe39 and with switch II residues Leu69, Leu72, and Pro75. A close inspection of the structural changes that accompany the exchange of GDP for GppNHp on RhoC helps to explain why the γ-phosphate is important for generating the effector-binding surface (Figure 6). In particular, upon the binding of GppNHp, both Gln63 and Tyr66 within the switch II region of RhoC assume the proper position for interactions with Lys100 from mDia1. In addition, the phenolic ring from Tyr66 of RhoC undergoes hydrophobic interactions with Leu96 from mDia1 (Figure 6a). The switch II movement that accompanies GDP−GppNHp exchange also reduces any steric hindrance between Asp65 and portions of mDia1 (Figure 6b) and brings Asp67 and Arg68 into position to undergo electrostatic interactions with Asn164 and Asn165, as well as with Asn166 and Asn217 of mDia1 (Figure 6c).

The fact that switch I minimally contributes to the binding interface for mDia1 leads us to propose that the RhoC−GppNHp structure, in which switch I still assumes the same conformation seen in the GDP-bound form of RhoC (i.e., pulled away from the guanine nucleotide) but where switch II has moved toward the γ-phosphate, represents a partially activated state. This form of RhoC is still able to bind mDia1, with the switch I region folding down so that residues Val38, Phe39, and Glu40 are positioned to interact with the effector protein (Figure 6d). We further propose that the structure obtained for the RhoC−GTPγS complex, where both switch I and switch II are brought into position to interact with the effector, represents the fully activated state.

DISCUSSION

The Two Activated States of RhoC: Implications for Effector Binding. The switch regions refer to the conformationally sensitive portions of GTPases that typically undergo structural changes upon GDP−GTP exchange, as first demonstrated for H-Ras (*32*, *33*). These structural changes are thought to represent the molecular basis for the activation of GTPases and their ability to recognize downstream target/effector proteins. The sequence of amino acid residues comprising switch I is fully conserved, when not identical, among the different members of the Rho family (*34*). In many of the cases where structures are available for the GTP-bound forms of Rho-related proteins, including RhoA (bound to GppNHp and GTPγS), RhoE (bound to GTP), Rac1 (bound to GppNHp), and Rnd1 (bound to GTP), the switch I loops superimpose well. In each of these examples, and similar to the structure for the RhoC−GTPγS complex, switch I is folded down toward the guanine nucleotide, enabling the conserved tyrosine residue (Tyr34 for RhoC) to be in hydrogen-bonding contact with the γ-phosphate.

Interestingly, the switch I loop does not follow the same pattern in the X-ray crystal structure for the RhoC−GppNHp

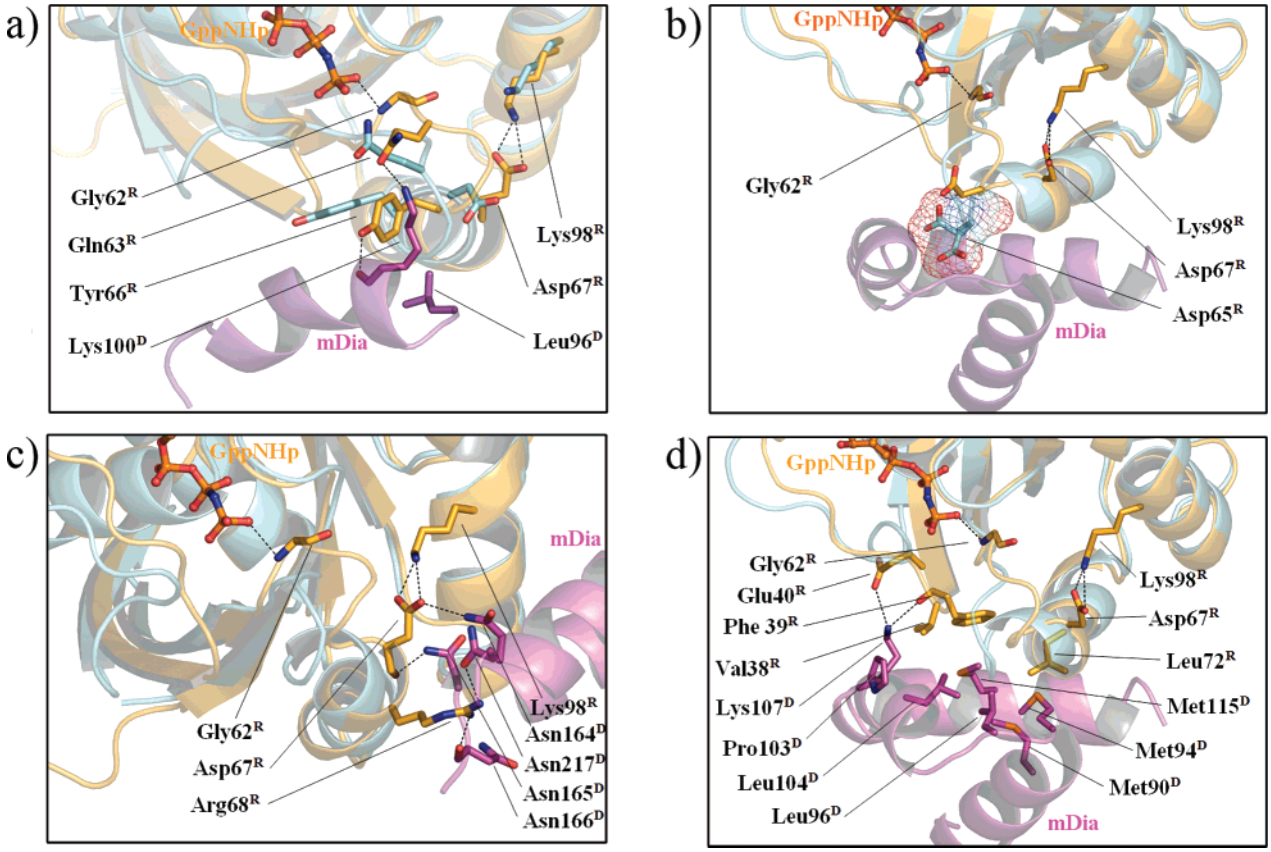

FIGURE 6: Conformational changes within the switch regions that occur upon the binding of GppNHp and the effector mDia1 to RhoC. Superposition between RhoC−GDP (cyan) and RhoC−GppNHp (orange) complexed to mDia1 (magenta, PDB ID 1Z2C). (a) The binding of GppNHp alters the positions of Gly62 and Asp67 of RhoC (indicated by R superscript) and brings Gln63 and Tyr66 of RhoC into suitable position to interact with Lys100 and Leu96 of mDia1 (indicated by D superscript). (b) The switch II movement is also important for preventing a steric clash between Asp65 of RhoC and the interaction surface of mDia1. (c) Asp67 and Arg68 of RhoC are brought into position to undergo electrostatic interactions with Asn164, Asn165, Asn166, and Asn217 of mDia1. (d) The switch I movement brings a hydrophobic stretch of RhoC residues ($Val38^R$ and $Phe39^R$), complemented by switch II residue $Leu72^R$, into position to interact with a hydrophobic core of residues within mDia1 (Met90, Met94, Leu96, Pro103, Leu104, and Met115). This hydrophobic contact is stabilized by the salt bridge between Lys107 of mDia1, and Phe39 and Glu40 (main chain and side chain, respectively) of RhoC.

complex, as it is pulled away from the guanine nucleotide. Within this conformation, Tyr34 is not in position to form a hydrogen bond with the γ-phosphate and Phe39 is trapped by an internal hydrophobic contact with Ile23 (Figure 4a). This in fact appears to be similar to what was reported for the X-ray crystal structure for the GppNHp-bound form of TC10 (*34*). Within the TC10 structure (PDB ID 2ATX), a conserved phenylalanine within switch I, equivalent to Phe39 in RhoC, is folded against a methionine side chain at a position equivalent to Ile23 in RhoC, which pulls switch I away from the guanine nucleotide. This unusual switch I position appears to have functional consequences, as TC10 has a significantly lower binding affinity for WASP (Wiscott Aldrich Syndrome Protein), compared to Cdc42 (*34*). A careful comparison of the X-ray structure for TC10 with the NMR structure for the Cdc42−WASP complex (*35*) highlights a structural mismatch between the WASP-interacting residues on Cdc42 (Val36−Asp38) and the corresponding region for TC10 (residues Val50−Asp52). As the switch I loop of TC10 is pulled up in relation to the switch I region for Cdc42 when complexed to WASP, these residues within TC10 are in positions that are not conducive to interactions with the effector (not shown). In order for a proper interaction to occur between activated TC10 and WASP, the switch I domain needs to be brought down toward the guanine nucleotide.

Another interesting example regarding the switch I fold comes from the highly related H-Ras and M-Ras proteins. The structure for the switch I loop of the M-Ras−GppNHp complex (*36*) is distinct from that for H-Ras crystallized with either GTP or various GTP analogues (*37*−*40*), as it is characterized by the complete loss of an interaction between Thr45 and the γ-phosphate (*36*). On the other hand, electron paramagnetic resonance and ^{31}P NMR studies of the H-Ras−GppNHp complex suggested that the coordination of Thr35 (equivalent to Thr45 in M-Ras) to the γ-phosphate is transient both in solution and in the crystalline state and that some population of H-Ras is incapable of this interaction (*41*−*43*). It was demonstrated by NMR spectroscopy that switch I adopts two different conformations within the H-Ras−GppNHp complex, designated as state 1 (off) and state 2 (on), with state 2 being more naturally abundant than state 1 (*44*). In addition, the binding of effector proteins induced a conversion of state 1 to state 2 (*44*−*46*). An examination of various H-Ras mutants suggested that the two states corresponded to distinct conformations for switch I, with Tyr32 (equivalent to Tyr34 in RhoA and RhoC) existing in two different positions depending on the bound guanine nucleotide (*44*). Studies using ^{31}P NMR indicated that M-Ras−GppNHp predominantly existed as a state 1 conformation in solution, with the gradual addition of c-Raf-1 then inducing a transition to state 2 (*36*). M-Ras is known

to exhibit a weak binding affinity for some Ras effectors, including c-Raf-1. Because M-Ras shares an identical effector region with H-Ras, it was proposed that the differences exhibited by these two proteins in their switch I conformation could explain their different affinities for target/effector proteins (*36*).

The two switch I states for RhoC that are described in this report likely represent distinct conformational transitions that occur in solution, as there are no crystalline contacts trapping switch I in its position in the RhoC−GppNHp complex (not shown). The majority of its residue positions are well defined because of the different interactions that they undergo. Some of these interactions involve the nitrogen base and phosphate moieties of the GTP analogue, and others represent intramolecular contacts that are apparently important for the stabilization of this partially activated state (e.g., Val38 to Cβ of Asp59, Phe30 to Ile23, and Ile43 to the main-chain carbons of the neighboring β-strand). The residues with poor electron density include Tyr34, which does not interact (through hydrogen bonding) with the γ-phosphate and is not involved in crystalline contacts.

The RhoC−GTPγS complex does show a crystalline contact within switch I. The binding of GTPγS in effect recruits more residues from switch I to the nucleotide-binding site (compare panels a and b of Figure 2). As a consequence, Phe39 no longer interacts with Ile23, but instead it is accommodated within a hydrophobic pocket provided through crystalline contacts. Likewise, in the complex containing RhoC−GppNHp and its effector mDia1, the initial engagement of the effector via switch II of the RhoC−GppNHp species allows switch I residues Val38 and Phe39 to seek a binding pocket within the effector protein.

It is interesting to note that RhoA was also crystallized bound to the same GTP analogues used here, and in those cases, switch I was identically positioned: folded down toward the guanine nucleotide, allowing it to make contact with the γ-phosphate through Tyr34 (Figure 4a). The RhoA−GppNHp and RhoA−GTPγS complexes (PDB ID 1KMQ and 1A2B, respectively) were crystallized in the same space group, with similar cell parameters. In each case, switch I makes crystalline contacts with helix A4 from a symmetry-related molecule. When the RhoC−GppNHp structure is superposed onto these RhoA structures, it appears that switch I, as presented in what we refer to as the partially activated state for the RhoC−GppNHp complex, could be accommodated within the crystalline packing of the RhoA proteins. Thus, there is not an obvious indication that the crystalline packing of the known RhoA crystal structures interferes with their ability to access an intermediate (partially activated) conformation.

To our knowledge, this represents the first demonstration of an alternative "active" state for RhoC. We believe that this alternative switch I conformation is able to bind to the effector protein mDia1, as only 3 of the 15 residues are pulled way from the effector contact site, and may be brought into proper position upon the binding of the effector. The available X-ray crystal structures for GTPγS-bound RhoA complexed to PKN (*47*) and GppNHp-bound RhoA complexed to ROCK (*48*) suggest that the switch II residues are responsible for most of the GTPase−effector contacts (not shown). If indeed RhoA does not exhibit an alternative GTP-bound state, then the differences in the switch I conformational folds exhibited by RhoA and RhoC may account for their distinct effector-binding capabilities. Both of these Rho proteins share extensive sequence similarity (around 85%) but show differences in their binding affinities for several effector proteins as indicated through yeast two-hybrid approaches and GST pull-down assays (*2*). Intriguingly, one of the differences between RhoA and RhoC is the substitution of a valine in RhoA (Val43) for an isoleucine in RhoC (Ile43), positioned near the switch I loop. The alternative switch I conformation exhibited by the RhoC−GppNHp complex has a shortened β2-strand and a longer switch I loop (Figure 4b); Ile43 in RhoC lies at the beginning of the β2-strand. It is apparent from the structure for RhoC−GppNHp that the β2-strand is pulled away relative to its position in the RhoC−GTPγS (Figure 4b) and RhoA−GTP complexes, with Ile43 being involved in hydrophobic interactions with residues from the neighboring β-strand (Figure 4b, see arrow). The larger bulk of the isoleucine side chain relative to valine might allow for a greater degree of interaction with these neighboring residues and perhaps helps to stabilize this alternative conformational state for RhoC.

Another interesting difference between the fully activated (GTPγS-bound) state for RhoC and its inactive (GDP-bound) and partially activated (GppNHp-bound) conformations is the considerable movement within the insert loop segment. While the functional implications of the observed changes in the insert loop of RhoC are not yet known, it is interesting that similar movements are not seen with RhoA (Figure 5). Effector proteins that uniquely interact with the insert loop of RhoA, RhoB, or RhoC have not been identified, although deletion of the insert domain of RhoA causes a decrease in protein stability and a reduction in its transforming potential (*14*) by decreasing its ability to activate Rho kinase (*15*). Thus, structural changes occurring within the insert loop could provide an additional mechanism by which RhoC and RhoA might trigger distinct signaling outcomes.

The Two Activated States of RhoC: Implications for Intrinsic GTPase Activity and Regulator Binding. When comparing the structures for the two activated states of RhoC, there appears to be differences in the position of the potential catalytic water for the GTPase reaction. The structure for RhoC in the fully activated state (i.e., bound to GTPγS and with both switch domains moved toward the GTP analogue) has the water correctly positioned for nucleophilic attack. In particular, it is a suitable distance from the γ-phosphate where it makes hydrogen bond contacts with Thr37, Gly62, and Gln63, similar to what has been observed in several catalytically active GTPases (Figure 3a). Previous studies have suggested that the conserved threonine residue in the switch I domain (e.g., Thr35 in Ras) plays an important role in the mechanism of GTP hydrolysis (*38*, *49*). Within the structure for the partially activated RhoC (i.e., bound to GppNHp), the position of switch I is altered, such that Thr37 can still interact with Mg^{2+} but it is unable to form a hydrogen bond with the catalytic water. The water is displaced relative to the γ-phosphate, and consequently it is not within catalytic position (Figure 3b). Therefore, this raises an interesting scenario, in which the fully activated form of RhoC is capable of an intrinsic GTPase activity, whereas the partially activated form would need to undergo a conformational change within switch I in order to direct Thr37 into the proper position for catalysis. GTPase-

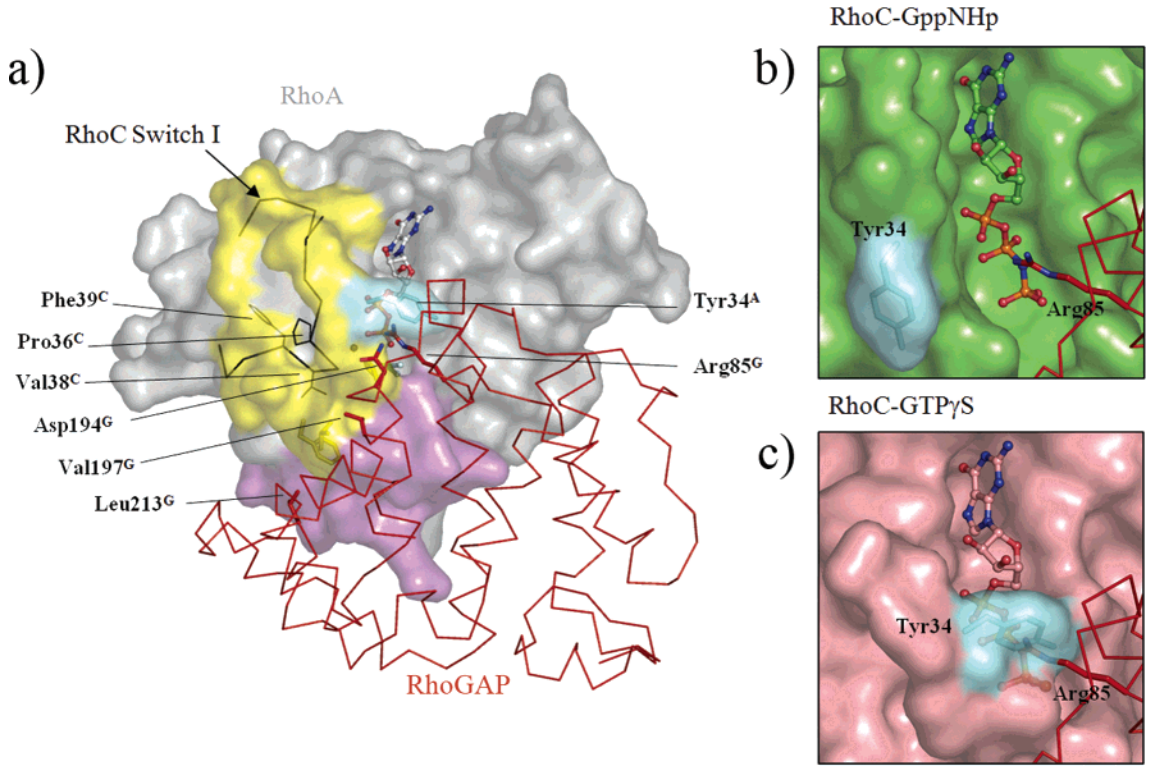

FIGURE 7: Implications for the GTP hydrolytic reaction. (a) The interaction of RhoA, presented as a surface (yellow for switch I, magenta for switch II, and gray for the remainder of the protein), with RhoGAP (*49*, PDB ID 1OW3), represented by a ribbon in red. Switch I residues Pro36, Val38, and Phe39 of RhoC−GppNHp (indicated by C superscript) are depicted to interact with RhoGAP (based on superposition with the X-ray structure for the RhoA−RhoGAP complex where the corresponding residues for RhoA are colored in yellow and represented by sticks). Residues of RhoGAP that are thought to be important for binding switch I are highlighted as sticks (Asp194, Val197, Leu213, superscript G for RhoGAP). The rest of the contact area is not depicted but involves mainly the switch II region. (b) The partially activated conformation of RhoC has better accessibility to the arginine finger of RhoGAP than does the fully activated (GTPγS-bound) conformation of RhoC. (c) In the fully activated state, Tyr34 of RhoC moves toward the γ-phosphate near the site of entry of the arginine finger of the RhoGAP (Arg85), as shown by superposing the structure for the RhoA−RhoGAP complex with the RhoC−GTPγS complex.

activating proteins (GAPs) appear to bind RhoA in a very similar fashion to effectors. For example, the RhoA−RhoGAP interface contains several switch II residues together with the switch I residues Pro36, Val38, and Phe39 (*50*). These same residues are pulled away from the contact area for the GAP when RhoC is in the partially activated state (Figure 7a). However, the binding of a GAP to this state of RhoC could bring switch I down into a catalytically competent conformation (with Thr37 being correctly positioned). Interestingly, the partially active conformation for RhoC might be more accessible to the catalytically essential arginine residue of the GAP (i.e., the "arginine finger"), as switch I within the partially activated state is not shielding the γ-phosphate (compare panels b and c of Figure 7). It may be that the partially activated state allows for a more effective GAP-promoted deactivation of RhoC molecules that are not involved in binding effectors and signal propagation.

Influence of GTP Analogues on the Activation of RhoC. It is always a question regarding how far one can take the interpretations made from structural and biochemical studies of the binding of GTPases to different GTP analogues. Indeed, the crystals for RhoC bound to GppNHp and GTPγS were obtained at different pH values (pH 6.4 and 4.8, respectively) raising the question of whether the distinct conformational states observed for these two nucleotide-bound forms of the GTPase might be the result of different crystallization conditions. However, we feel that this is unlikely to be the case as the critical determinant of the switch I conformational change appears to be a hydrogen-bonding interaction between the γ-phosphate group of the GTP analogue and Tyr34 and a hydrophobic contact between the sulfur atom (of GTPγS) and Pro36. The pH for the crystallization conditions of both RhoC−GppNHp and RhoC−GTPγS was significantly below the pK_a for tyrosine (10.13), suggesting that, in each case, Tyr34 has the potential for making a hydrogen bond with the γ-phosphate. The two activated conformational states for H-Ras and M-Ras, as detected by ^{31}P NMR, showed Tyr32 (equivalent to Tyr34 in Rho subfamily) to be in different positions relative to the bound nucleotide and were observed both with GTP and GTP analogues (*44*). Likewise, an important difference between the two activated states for RhoC described in this study is the positioning of Tyr34 in relation to the γ-phosphate of GTP. For the partially activated state, Tyr34 is not within hydrogen-bonding distance to the γ-phosphate, whereas it is in the fully activated state (Figure 4c). A comparison between GTP, GppNHp, and GppCH$_2$p showed that, for the free nucleotides in solution, the pK_a values for the γ-phosphate group increase from 6.3/4.7 for GTP/Mg^{2+}·GTP to 8.9/6.3 for GppNHp/Mg^{2+}·GppNHp and 9.0/6.6 for GppCH$_2$p/Mg^{2+}·GppCH$_2$p (*51*). Thus, one might expect that the pK_a values for the γ-phosphate groups of the GTP analogues are more than 2 units higher than the corresponding value for

GTP, thereby implying a decreasing capacity for accepting a hydrogen bond from the phenol ring of Tyr32. In this way, the use of GppNHp for RhoC crystallization might favor trapping a more open switch I structure. A variety of initial crystallization conditions were obtained for RhoC−GppNHp, which could be related to the presence of a number of switch conformations in solution.

On the other hand, crystals were only obtained for one condition for the RhoC−GTPγS complex, thus suggesting that this GTP analogue most likely favored the stabilization of a closed switch I conformation that has Tyr34 in proximity to the γ-phosphate. Figure 2b shows that, besides the hydrogen bond between the γ-phosphate sulfur and Tyr34, the sulfur makes a hydrophobic contact with another residue from switch I, namely, Pro36. Given that H-Ras has a conserved proline (Pro34) at the corresponding position, it is interesting that the use of GTPγS in ^{31}P NMR experiments with H-Ras abolished the state 1 (off) conformation, such that only state 2 (on) was detected.

CONCLUSIONS

In conclusion, we present here the X-ray crystal structures for RhoC bound to GDP and two GTP analogues, GppNHp and GTPγS. Comparisons between the GDP and GTP analogue bound forms of the protein reveal two activated states for RhoC. The partially activated state (obtained from the complex with GppNHp) shows the displacement of switch II toward the γ-phosphate, a movement that places several residues in the proper position to make important contacts with the effector mDia1. Switch I within the partially activated state is in essentially the same position as it is in the GDP-bound state, such that it is pulled away from the guanine nucleotide. The fully activated state (crystallized in the presence of GTPγS) shows that both switch I and switch II are displaced relative to their positions in the GDP-bound conformation. Switch I is positioned such that it is folded down toward the guanine nucleotide, allowing Tyr34 to make a hydrogen bond with the γ-phosphate. In this conformation, the intramolecular contact between Phe39 and Ile23 is broken, exposing the phenylalanine to the surface, along with Val38 and Glu40. Each of these residues is an important contributor to the effector-binding surface. By analogy to what has been described for H-Ras and M-Ras, we propose that these two activated states for RhoC exist as distinct populations in equilibrium. The partially activated state, similar to the state 1 conformation for Ras, seems to be catalytically compromised with regard to GTP hydrolytic activity, at least in the absence of a GAP, and therefore might represent a more "long-lived" activated state that can then be converted to a fully activated state (analogous to state 2 for Ras) in the presence of an effector. RhoA, which belongs to the same family and shares several effectors with RhoC, was crystallized only in the fully activated conformation. Thus, the distinct switch I structures between RhoA and Rho C might account for their reported differences in effector interactions. However, future studies involving ^{31}P NMR might shed further light on whether indeed RhoA does not adopt an intermediate or partially activated state, as well as potentially highlight how effector proteins distinguish between the activated conformation(s) of RhoA versus those of RhoC.

ACKNOWLEDGMENT

We thank Andre Ambrosio for help with the crystallographic analysis, Mario Sanches for helpful discussion, and Cindy Westmiller for excellent secretarial service.

REFERENCES

1. Ridley, A. J., Schwartz, M. A., Burridge, K., Firtel, R. A., Ginsberg, M. H., Borisy, G., Parsons, J. T., and Horwitz, A. R. (2003) Cell migration: integrating signals from front to back, *Science 302*, 1704−1709.
2. Wheeler, A. P., and Ridley, A. J. (2004) Why three Rho proteins? RhoA, RhoB, RhoC, and cell motility, *Exp. Cell Res. 301*, 43−49.
3. Sahai, E., and Marshall, C. J. (2002) RHO-GTPases and cancer, *Nat. Rev. Cancer 2*, 133−142.
4. Khosravi-Far, R., Solski, P. A., Clark, G. J., Kinch, M. S., and Der, C. J. (1995) Activation of Rac1, RhoA, and mitogen-activated protein kinases is required for Ras transformation, *Mol. Cell. Biol. 15*, 6443−6453.
5. Lebowitz, P. F., Davide, J. P., and Prendergast, G. C. (1995) Evidence that farnesyltransferase inhibitors suppress Ras transformation by interfering with Rho activity, *Mol. Cell. Biol. 15*, 6613−6622.
6. del Peso, L., Hernádez-Alcoceba, R., Embade, N., Carnero, A., Esteve, P., Paje, C., and Lacal, J. C. (1997) Rho proteins induce metastatic properties in vivo, *Oncogene 15*, 3047−3057.
7. Wu, M., Wu, Z. F., Kumar-Sinha, C., Chinnaiyan, A., and Merajver, S. D. (2004) RhoC induces differential expression of genes involved in invasion and metastasis in MCF10A breast cells, *Breast Cancer Res. Treat. 84*, 3−12.
8. Clark, E. A., Golub, T. R., Lander, E. S., and Hynes, R. O. (2000) Genomic analysis of metastasis reveals an essential role for RhoC, *Nature 406*, 532−535.
9. Fujisawa, K., Fujita, A., Ishizaki, T., Saito, Y., and Narumiya, S. (1996) Identification of the Rho-binding domain of p160ROCK, a Rho-associated coiled-coil containing protein kinase, *J. Biol. Chem. 271*, 23022−23028.
10. Sahai, E., and Marshall, C. J. (2002) ROCK and Dia have opposing effects on adherens junctions downstream of Rho, *Nat. Cell Biol. 4*, 408−415.
11. Riento, K., and Ridley, A. J. (2003) Rocks: multifunctional kinases in cell behaviour, *Nat. Rev. Mol. Cell Biol. 4*, 446−456.
12. Allal, C., Favre, G., Couderc, B., Salicio, S., Sixou, S., Hamilton, A. D., Sebti, S. M., Lajoie-Mazenc, I., and Pradines, A. (2000) RhoA prenylation is required for promotion of cell growth and transformation and cytoskeleton organization but not for induction of serum response element transcription, *J. Biol. Chem. 275*, 31001−31008.
13. Stamatakis, K., Cernuda-Morollón, E., Hernández-Perera, O., and Pérez-Sala, D. (2002) Isoprenylation of RhoB is necessary for its degradation. A novel determinant in the complex regulation of RhoB expression by the mevalonate pathway, *J. Biol. Chem. 277*, 49389−49396.
14. Zong, H., Raman, N., Mickelson-Young, L. A., Atkinson, S. J., and Quilliam, L. A. (1999) Loop 6 of RhoA confers specificity for effector binding, stress fiber formation, and cellular transformation, *J. Biol. Chem. 274*, 4551−4560.
15. Zong, H., Kaibuchi, K., and Quilliam, L. A. (2001) The insert region of RhoA is essential for Rho kinase activation and cellular transformation, *Mol. Cell. Biol. 21*, 5287−5298.
16. Rose, R., Weyand, M., Lammers, M., Ishizaki, T., Ahmadian, M. R., and Wittinghofer, A. (2005) Structural and mechanistic insights into the interaction between Rho and mammalian Dia, *Nature 435*, 513−518.
17. Leslie, A. G. W. (1992) *Jt. CCP4 + ESF-EAMCB Newsl. Protein Crystallogr.*, No. 26.
18. Evans, P. R. (1993) Proceedings of CCP4 Study Weekend, on Data Collection & Processing, Jan 9−10, Daresbury, U.K., pp 114−122, Daresbury Laboratory, Daresbury, U.K.
19. Vagin, A., and Teplyakov, A. (1997) MOLREP: an automated program for molecular replacement, *J. Appl. Crystallogr. 30*, 1022−1025.
20. Matthews, B. M. (1968) Solvent content of protein crystals, *J. Mol. Biol. 33*, 491−497.

21. Murshudov, G. N., Vagin, A. A., and Dodson, E. J. (1997) Refinement of macromolecular structures by the maximum-likelihood method, *Acta Crystallogr. D53*, 240−255.
22. Emsley, P., and Cowtan, K. (2004) Coot: model-building tools for molecular graphics, *Acta Crystallogr. D60*, 2126−2132.
23. Laskowski, R. A., MacArthur, M. W., Moss, D. S., and Thornton, J. M. (1993) PROCHECK: a program to check the stereochemical quality of protein structures, *J. Appl. Crystallogr. 26*, 283−291.
24. Kabsch, W. (1976) A solution for the best rotation to relate two sets of vectors, *Acta Crystallogr. A32*, 922−923.
25. Ihara, K., Muraguchi, S., Kato, M., Shimizu, T., Shirakawa, M., Kuroda, S., Kaibuchi, K., and Hakoshimai, T. (1998) Crystal structure of human RhoA in a dominantly active form complexed with a GTP analogue, *J. Biol. Chem. 273*, 9656−9666.
26. Pai, E. F., Krengel, U., Petsko, G. A., Goody, R. S., Kabsch, W., and Wittinghofer, A. (1990) Refined crystal structure of the triphosphate conformation of H-ras p21 at 1.35 Å resolution: implications for the mechanism of GTP hydrolysis, *EMBO J. 9*, 2351−2359.
27. Tarricone, C., Xiao, B., Justin, N., Walker, P. A., Rittinger, K., Gamblin, S. J., and Smerdon, S. J. (2001) The structural basis of Arfaptin-mediated cross-talk between Rac and Arf signalling pathways, *Nature 411*, 215−219.
28. Rudolph, M. G., Wittinghofer, A., and Vetter, I. R. (1999) Nucleotide binding to the G12V-mutant of Cdc42 investigated by X-ray diffraction and fluorescence spectroscopy: two different nucleotide states in one crystal, *Protein Sci. 8*, 778−787.
29. Hall, B. E., Bar-Sagi, D., and Nassar, N. (2002) The structural basis for the transition from Ras-GTP to Ras-GDP, *Proc. Natl. Acad. Sci. U.S.A. 99*, 12138−12142.
30. Wei, Y., Zhang, Y., Derewenda, U., Liu, X., Minor, W., Nakamoto, R. K., Somlyo, A. V., Somlyo, A. P., and Derewenda, Z. S. (1997) Crystal structure of RhoA-GDP and its functional implications, *Nat. Struct. Biol. 4*, 699−703.
31. Longenecker, K., Read, P., Lin, S. K., Somlyo, A. P., Nakamoto, R. K., and Derewenda, Z. S. (2003) Structure of a constitutively activated RhoA mutant (Q63L) at 1.55 Å resolution, *Acta Crystallogr. D59*, 876−880.
32. Pai, E. F., Kabsch, W., Krengel, U., Holmes, K. C., John, J., and Wittinghofer, A. (1989) Structure of the guanine-nucleotide-binding domain of the Ha-ras oncogene product p21 in the triphosphate conformation, *Nature 341*, 209−214.
33. Milburn, M. V., Tong, L., deVos, A. M., Brunger, A., Yamaizumi, Z., Nishimura, S., and Kim, S. H. (1990) Molecular switch for signal transduction: structural differences between active and inactive forms of protooncogenic ras proteins, *Science 247*, 939−945.
34. Hemsath, L., Dvorsky, R., Fiegen, D., Carlier, M. F., and Ahmadian, M. R. (2005) An electrostatic steering mechanism of Cdc42 recognition by Wiskott-Aldrich syndrome proteins, *Mol. Cell 20*, 313−324.
35. Abdul-Manan, N., Aghazadeh, B., Liu, G. A., Majumdar, A., Ouerfelli, O., Siminovitch, K. A., and Rosen, M. K. (1999) Structure of Cdc42 in complex with the GTPase-binding domain of the "Wiskott-Aldrich syndrome" protein, *Nature 399*, 379−383.
36. Ye, M., Shima, F., Muraoka, S., Liao, J., Okamoto, H., Yamamoto, M., Tamura, A., Yagi, N., Ueki, T., and Kataoka, T. (2005) Crystal structure of M-Ras reveals a GTP-bound "off" state conformation of Ras family small GTPases, *J. Biol. Chem. 280*, 31267−31275.
37. Hall, B. E., Bar-Sagi, D., and Nassar, N. (2002) The structural basis for the transition from Ras-GTP to Ras-GDP, *Proc. Natl. Acad. Sci. U.S.A. 99*, 12138−12142.
38. Scheidig, A. J., Burmester, C., and Goody, R. S. (1999) The pre-hydrolysis state of p21(ras) in complex with GTP: new insights into the role of water molecules in the GTP hydrolysis reaction of ras-like proteins, *Structure 7*, 1311−1324.
39. Schweins, T., Scheffzek, K., Assheuer, R., and Wittinghofer, A. (1997) The role of the metal ion in the p21ras catalysed GTP-hydrolysis: Mn^{2+} versus Mg^{2+}, *J. Mol. Biol. 266*, 847−856.
40. Pai, E. F., Krengel, U., Petsko, G. A., Goody, R. S., Kabsch, W., and Wittinghofer, A (1990) Refined crystal structure of the triphosphate conformation of H-ras p21 at 1.35 Å resolution: implications for the mechanism of GTP hydrolysis, *EMBO J. 9*, 2351−2359.
41. Bellew, B. F., Halkides, C. J., Gerfen, G. J., Griffin, R. G., and Singel, D. J. (1996) High frequency (139.5 GHz) electron paramagnetic resonance characterization of Mn(II)-$H_2{}^{17}O$ interactions in GDP and GTP forms of p21 ras, *Biochemistry 35*, 12186−12193.
42. Halkides, C. J., Bellew, B. F., Gerfen, G. J., Farrar, C. T., Carter, P. H., Ruo, B., Evans, D. A., Griffin, R. G., and Singel, D. J. (1996) High frequency (139.5 GHz) electron paramagnetic resonance spectroscopy of the GTP form of p21 ras with selective 17O labeling of threonine, *Biochemistry 35*, 12194−12200.
43. Iuga, A., Spoerner, M., Kalbitzer, H. R., and Brunner, E. (2004) Solid-state 31P NMR spectroscopy of microcrystals of the Ras protein and its effector loop mutants: comparison between crystalline and solution state, *J. Mol. Biol. 342*, 1033−1040.
44. Geyer, M., Schweins, T., Herrmann, C., Prisner, T., Wittinghofer, A., and Kalbitzer, H. R. (1996) Conformational transitions in p21ras and in its complexes with the effector protein Raf-RBD and the GTPase activating protein GAP, *Biochemistry 35*, 10308−10320.
45. Spoerner, M., Herrmann, C., Vetter, I. R., Kalbitzer, H. R., and Wittinghofer, A. (2001) Dynamic properties of the Ras switch I region and its importance for binding to effectors, *Proc. Natl. Acad. Sci. U.S.A. 98*, 4944−4949.
46. Linnemann, T., Geyer, M., Jaitner, B. K., Block, C., Kalbitzer, H. R., Wittinghofer, A., and Herrmann, C. (1999) Thermodynamic and kinetic characterization of the interaction between the Ras binding domain of AF6 and members of the Ras subfamily, *J. Biol. Chem. 274*, 13556−13562.
47. Maesaki, R., Ihara, K., Shimizu, T., Kuroda, S., Kaibuchi, K., and Hakoshima, T. (1999) The structural basis of Rho effector recognition revealed by the crystal structure of human RhoA complexed with the effector domain of PKN/PRK1, *Mol. Cell 4*, 793−803.
48. Dvorsky, R., Blumenstein, L., Vetter, I. R., and Ahmadian, M. R. (2004) Structural insights into the interaction of ROCKI with the switch regions of RhoA, *J. Biol. Chem. 279*, 7098−7104.
49. Pai, E. F., Krengel, U., Petsko, G. A., Goody, R. S., Kabsch, W., and Wittinghofer, A. (1990) Refined crystal structure of the triphosphate conformation of H-ras p21 at 1.35 Å resolution: implications for the mechanism of GTP hydrolysis, *EMBO J. 9*, 2351−2359.
50. Graham, D. L., Lowe, P. N., Grime, G. W., Marsh, M., Rittinger, K., Smerdon, S. J., Gamblin, S. J., and Eccleston, J. F. (2002) $MgF_3{}^-$ as a transition state analog of phosphoryl transfer, *Chem. Biol. 9*, 375−381.
51. Spoerner, M., Nuehs, A., Ganser, P., Herrmann, C., Wittinghofer, A., and Kalbitzer, H. R. (2005) Conformational states of Ras complexed with the GTP analogue GppNHp or GppCH2p: implications for the interaction with effector proteins, *Biochemistry 44*, 2225−2236.
52. DeLano, W. L. (2002) The PyMOL Molecular Graphics System, DeLano Scientific, San Carlos, CA.

BI700035P